Xin Li[1]
Ting-Jie Wang[1]
Yong Jin[1]

[1] Department of Chemical Engineering, Tsinghua University, Beijing, China.

Research Article

Granulation Process for Producing Spherical Particles of a Rubber Antioxidant in a Water Cooling Tower

A new granulation technology for producing spherical particles of a rubber antioxidant and its key factors were studied. The granulation is based on the interfacial tension and immiscibility of the rubber antioxidant in water. Melted antioxidant was ejected from nozzles to form drops in air that fell into a water tower where they were cooled and solidified into spherical particles as they fell. After dewatering and air drying, spherical particles with a uniform size were obtained. Experiments performed on the granulation of antioxidant 4020 are described and the key factors, including falling height, drop temperature and surfactant concentration in water were studied. The mechanism of drop entrancement in water was analyzed and the stable operating conditions were investigated. The technology produces spherical particles with a uniform size using smaller equipment and is also suitable for producing spherical particles from other melted materials with similar physical properties.

Keywords: Granulation process, Particles, Rubber antioxidant

Received: January 18, 2006; *revised:* June 4, 2006; *accepted:* June 8, 2006

DOI: 10.1002/ceat.200600023

1 Introduction

Rubber antioxidants are widely used in various rubber products to prevent them from getting oxidized and extend their lives. Antioxidants 4020 (6PPD, $C_{18}H_{29}N_2$) and 4010NA (IPPD, $C_{15}H_{18}N_2$), usually used in tyres and shoes, are very common and have the largest output and consumption [1].

The granulation of the rubber antioxidant is very important in its application. On the one hand, it can reduce the dust in the production to give a better environment. On the other hand, it can improve the fluidity, dispersibility, and mixing uniformity of the material, thus improving the quality of the rubber products and satisfying the requirements for automatic feeding in the production line. Also, granulation makes packing, storage, transportation and application of the products much more convenient and cheaper [2].

The current granulation technology for rubber antioxidants is wax-flake molding with a belt cooler [3]. In this technology, melted feed is dropped onto a moving belt of stainless steel from a rotating drum, and cooling water is sprayed onto the back surface of the belt. The drops are cooled and solidified on the moving belt. Subsequently, the cooled particles are scrapped off by a scraper. The flake particles have poor fluidity and dispersibility. The cooling efficiency is low due to the indirect heat transfer through the belt and a long belt of about 10 m is needed. The equipment has a complicated structure and many moving parts, resulting in a higher failure rate. Besides, particles easily adhere to the belt and the belt is easily worn out.

Fang et al. [3] reported a granulation process for producing spherical wax particles in a water cooling tower. The process makes use of the interfacial tension of melted wax in water as well as the immiscibility property between wax and water, which makes melted wax form discrete spherical drops from nozzles under the water. Since the wax density is lower than water, the drops rise in the water tower and are cooled and solidified in the rising process. The solidified particles are overflowed and air dried, and spherical particles are obtained. This technology can produce wax particles with a very spherical shape and uniform diameters, and it has a high cooling efficiency and simple equipment structure.

In this work, a new granulation technology for a rubber antioxidant basing on previous works [3, 4] was developed to produce spherical particles by direct cooling in water. The granulation flow of antioxidant 4020, and the mechanism and key factors of the drop entrancement process were studied.

Correspondence: T.-J. Wang (wangtj@mail.tsinghua.edu.cn), Department of Chemical Engineering, Tsinghua University, Beijing 100084, PR China.

2 Design of Granulation Flow

The molecular structures and main granulation properties of antioxidants 4020 and 4010NA are listed in Tab. 1. Both have similar properties. Antioxidant 4020 was used in this research for describing the granulation process and the key factors. The granulation flow for 4020 is shown in Fig. 1. The granulation material was stirred in a feed tank. Then, it was sent into a precrystallizer, which was used to produce crystal nuclei and to induce crystallization and solidification. 4020 and 4010NA are both typical materials with supercooling characteristics, which stay in the liquid phase or crystallize very slowly in the absence of nuclei even though the temperature is lower than the melting point. For example, if there is no nucleus, 4020 does not solidify even at a temperature below 0 °C. The feed will have a certain concentration of nuclei and can solidify in tens of seconds after passing through the precrystallizer. The precrystallizer is a known technology and is not discussed here. Then, the feed was sent into the granulator, controlled at a definite temperature and pressure, where it formed large numbers of discrete drops from the nozzles on the distributor. The drops fell down into the water tower from a falling height. As 4020 has a higher density than water and is immiscible in water, the drops sank in the water keeping their spherical shape and were cooled and solidified. The particles at the tower bottom were discharged along with the water flow. After they were dewatered through a vibrating screen, they were air dried in a fluidized bed. Since water was mainly adsorbed on the particle surface, the particles were easily dried. The water flow was pumped back to the tower after cooling.

The granulator is the key equipment in the granulation process. Discrete drops with a uniform diameter were formed through a nozzle distributor. Each nozzle on the distributor is designed to have the same pressure drop through the inner structure. Drops were formed from each nozzle at basically the same frequency. The temperature in the granulator should be well controlled as the crystal nuclei melt if it is too high or the granulator gets blocked if solidification was too fast if the temperature is too low. In the experiments, the temperature inside the granulator was usually controlled around the melting point and the nozzle temperature was controlled about 1–2 °C higher, which helps the feed flow and the drops form easily. The granulator was insulated on the outside to operate adiabatically.

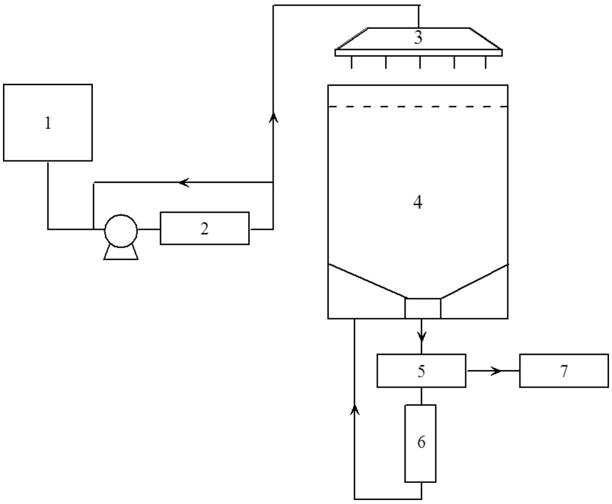

Figure 1. Granulation flow. 1) feed tank, 2) precrystallizer, 3) nozzle distributor, 4) water cooling tower, 5) dewatering screen, 6) cooler, 7) air drying.

Circulating water to the tower brings a slight upward flow through a distributor structure, loosening the particle stack at the tower bottom, which makes the particle discharge smoothly with the water. Any strong disturbance in the tower should be avoided to prevent collision and adhesion between falling drops. A fluidized bed was used for air drying of the particles and it performed very well. The water contained in the particles was reduced to trace levels only after 5 min residence time for particle drying in the fluidized bed.

Good spherical particles of 4020 and 4010NA with diameters of (4.0 ± 0.3) mm were produced in the experiments. The spherical particles are shown in Figs. 2 and 3. The granulation products of 4020 by wax-flake molding with a belt cooler are shown in Fig. 4 for comparison.

3 Process of Drop Entrancement in Water

The granulation process includes drop formation, drop entrancement in water, drop cooling and solidification in water and particle drying. The drops are formed through the nozzles on a distributor which produces discrete and uniform drops in

Table 1. Parameters for 4020 and 4010NA [1].

Feed brand	Molecular Structure	Density [g/cm^3]	Melting point [°C]	Viscosity [mPa/s] at melting point
4020	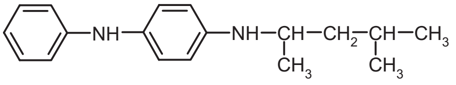	1.04	46	96.5
4010NA	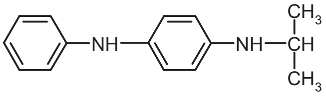	1.14	72	11.7

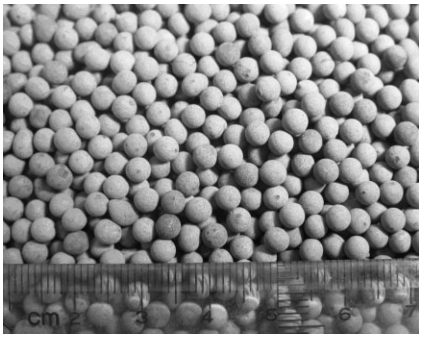

Figure 2. Spherical particles from new granulation process (4020).

Figure 3. Spherical particles from new granulation process (4010NA).

Figure 4. Product particles from wax-flake molding with a belt cooler (4020).

air. The drops fall and cool in the water due to the higher density of the drop. Particle dewatering and drying can also be easily accomplished in the laboratory and industry. The most complicated process is drop entrancement in water because of the small difference in density and interfacial tension of water and the antioxidant. The experiments showed that the drops often spread out or float on the water surface instead of entering the water. Therefore, drop entrancement is the most crucial step in this granulation process.

The experiments showed that the falling drops of 4020 often spread on the water surface like a thin oil film rather than entering the water, regardless of temperature and velocity. This is due to the hydrophobic properties of 4020 and the positive spreading coefficient. The spreading coefficient S is defined as:

$$S = \gamma_c - \gamma_p - \gamma_{cp} \tag{1}$$

where γ_c is the surface tension of the continuous phase (cooling medium, water), γ_p the surface tension of the dispersed phase (drop, melted antioxidant), and γ_{cp} the interfacial tension between the two phases. According to the Fowkes equation [5], γ_{cp} can be written as:

$$\gamma_{cp} = \gamma_c + \gamma_p - 2\sqrt{\gamma_c \gamma_p} \tag{2}$$

Combining Eqs. (1) and (2) yields:

$$S = 2\sqrt{\gamma_p}\left(\sqrt{\gamma_c} - \sqrt{\gamma_p}\right) \tag{3}$$

From Eq. (3), it can be seen that the spreading coefficient is positive when the surface tension of water is larger than that of the drop, which causes the drop to spread out. In the analysis, it is assumed that the temperature of the water at the drop interface is equal to the drop temperature. However, the surface tension of water is usually larger than that of 4020, e.g., at 46 °C:

$\gamma_c = 68.6$ mN/N, $\gamma_p = 34.9$ mN/m

Thus, the spreading phenomenon is spontaneous in this case. The spreading coefficient must be made negative to keep the drops spherical and get them to enter the water properly. It can be seen from Eq. (3) that this requires reducing the surface tension of water. The most convenient method is by adding a surfactant into the water.

3.1 Addition of Surfactant

For a rubber antioxidant system, the following points need to be considered in surfactant selection: (1) it should not be harmful to the function and properties of rubber and the rubber antioxidant; (2) it should reduce the water surface tension effectively; (3) it should produce little foam; (4) it should be degradable and environmentally benign; and (5) it should be cheap. Since the added amount of surfactant is small, the first four points are more important.

A fatty alcohol polyoxyethylene ether such as AEO7 [$R\text{-}O\text{-}(CH_2\text{-}CH_2\text{-}O)_7\text{-}H$, $R{=}C_{12}H_{25}\text{-}C_{14}H_{29}$] is a good choice for the surfactant. It is used in the rubber industry as a wetting reagent and produces less foam because of the nonionic structure, and the chain structure of the molecule is degradable [6]. It meets the requirements of this granulation process well. The following experiments were carried out with AEO7 as the surfactant.

The surface tension change as a function of the surfactant concentration was measured and shown in Fig. 5. It can be seen that when the concentration of AEO7 reaches about 10^{-5} mol/L, the surface tension of water is lower than that of the melted antioxidant. This is the minimum concentration of the surfactant in the water that gives a negative spreading coefficient. Fig. 5 also shows that the surface tension of water is stable after the surfactant concentration reaches about $0.5 \cdot 10^{-4}$ mol/L, which corresponds to the critical micelle concentration (CMC) of AEO7. If the surfactant concentration exceeds the CMC too much, too many surfactant micelles are formed that can dissolve the molecules of 4020, leading to the antioxidant pollution of the water. The experiments showed that the suitable concentration of AEO7 for antioxidant granulation is 10^{-5}–10^{-4} mol/L.

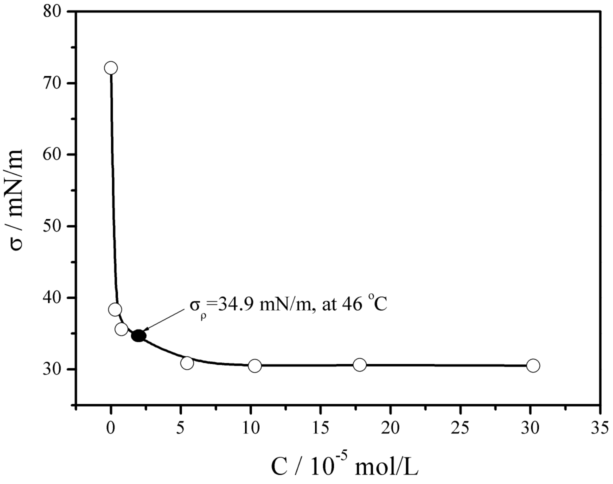

Figure 5. Surface tension of water vs AEO7 concentration.

There is a little loss of surfactant due to its adsorption on the particles in the air drying process. A surfactant supply is needed to keep the concentration of the surfactant in the water stable in a continuous granulation.

3.2 Critical Entrancement Height and Conditions

Although the drops do not spread out on the water surface after the reduction of the water surface tension to make the spreading coefficient negative through the addition of the surfactant, drop entrancement in the water is still not ensured. Another phenomenon named "lens" can occur in which the drop keeps floating on the water surface and looks like a lens from the side, as shown in Fig. 6. In this case, there are three forces acting on the drop in the vertical direction, i.e., gravity, buoyancy and the resultant force of surface and interfacial tensions. Due to that the density difference between water and 4020 is only 0.04 g/cm^3, the difference in gravity and buoyancy is easily balanced by the resultant force of the surface and interfacial tensions, causing the drops to float on the water surface. This is harmful and the design of the granulation process should take care to avoid this because floating drops can collide with subsequent falling drops and both of them can combine or break into many droplets. It was noticed in the experiments that drops with a shorter falling height tend to float while those with a longer falling height easily enter the water. Thus, a concept of critical entrancement height *Hc* can be defined, which is the falling height when the drop changes from one that floats on to one that enters the water. Experiments were carried out to investigate the relationship between *Hc* and other factors such as the drop temperature, AEO7 concentration, etc. for use in the granulation system design and operation. The experimental apparatus is shown in Fig. 7. The drops were obtained through a nozzle and the frequency of production was controlled by adjusting a valve. The feed temperature was controlled by circulating water with a constant temperature. The falling heights were adjusted by a little crane to determine the critical entrancement height at a specific drop temperature, initial velocity at the nozzle tip and surfactant concentration. The drop initial velocity at the nozzle tip was obtained by the analysis of pictures recorded by a video camera.

The change in the critical entrancement heights *Hc* with drop temperature at different concentrations is shown in Fig. 8. The *Hc* change with the surfactant concentration at different drop temperatures is shown in Fig. 9. It was noticed that *Hc* decreased as the drop temperature and surfactant concentration increased. Increasing either drop temperature or surfactant concentration will cause a decrease in the water surface tension, which lets the drop enter the water easily.

It was observed in the experiments that a bubble often appeared when the drop entered the water, and some bubbles ad-

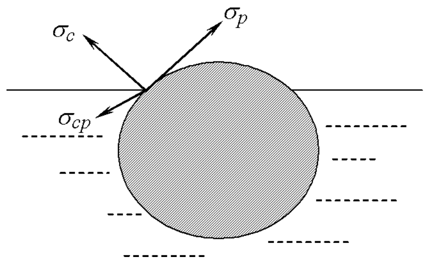

Figure 6. A lens-like drop floats on the water surface; σ_c water surface tension, σ_p drop surface tension, σ_{cp} interfacial tension between water and drop.

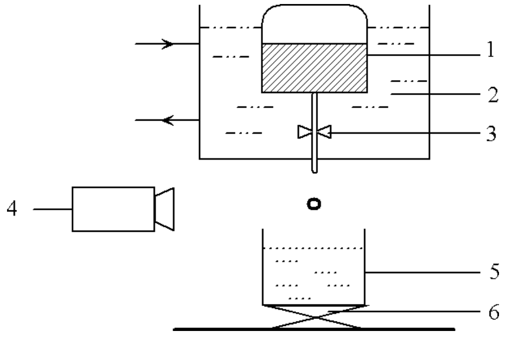

Figure 7. Apparatus for drop critical entrancement height measurement.
1 feed, 2 thermostat water, 3 valve, 4 video camera, 5 AEO7 solution, 6 crane for height adjustment

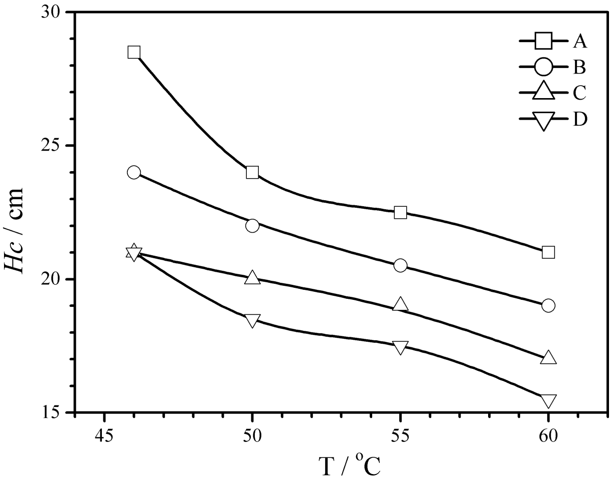

Figure 8. Critical entrancement height vs drop temperature. Surfactant concentrations (mol/L): A: $6.55 \cdot 10^{-6}$, B: $5.76 \cdot 10^{-5}$, C: $3.41 \cdot 10^{-4}$, D: $1.93 \cdot 10^{-3}$

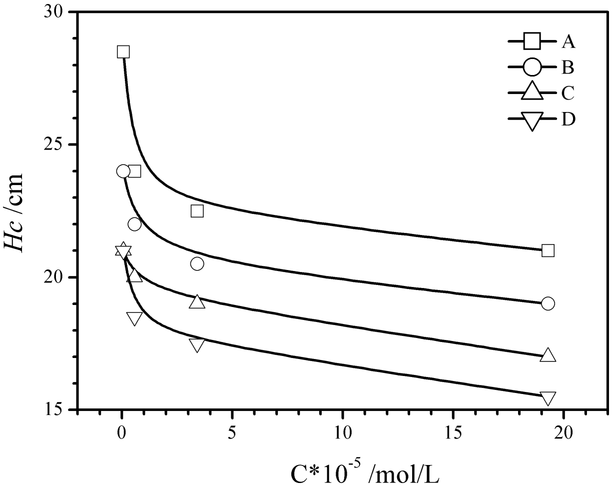

Figure 9. Critical entrancement height vs surfactant concentration. Drop temperature: A: 46 °C, B: 50 °C, C: 55 °C, D: 60 °C

hered to the upper surface of the drops, which caused those drops that had already entered the water to float up again. Oguz and Prosperetti [7] reported the conditions for underwater bubble formation, and Morton et al. [8] described the conditions and corresponding phenomena in three regions. The first is a "shallow crater region", with the conditions to form little craters on the water surface because of the low velocity of the drop. With increasing drop velocity there follows a "bubble entrainment region", where a bubble forms under water and the cavity is nearly semispherical. At a still higher drop velocity, a "broad jet region" appears where the cavity has a nearly cylindrical shape and is much larger than the cavities in the first two regions. The lower boundary of the bubble entrainment region can be fitted by a power function of We and Fr numbers:

$$\mathrm{We} = \alpha \mathrm{Fr}^{\beta} \tag{4}$$

where We is the Weber number, Fr is the Froude number, and α and β are fitted constants. For the case of a water drop, $\mathrm{We} = 41.3\mathrm{Fr}^{0.179}$ [8]. The We and Fr numbers are defined as below:

$$\mathrm{We} = \frac{\rho U^2 D}{\sigma} \tag{5}$$

$$\mathrm{Fr} = \frac{U^2}{gD} \tag{6}$$

The We and Fr numbers include the factors that determine the critical entrancement height, i.e., drop falling height, drop velocity, drop temperature and surfactant concentration. The drop temperature and surfactant concentration mainly affect the surface tension of water. The experimental results for critical entrancement are shown in Fig. 10. The experimental results were fitted in the form of a power function as:

$$\mathrm{We} = 23.5\mathrm{Fr}^{0.672} \tag{7}$$

The fitted curve is also shown in Fig. 10. The experimental points are fitted well except for a few points due to experimental errors. Drops under the conditions above the curve can enter the water easily, while those below the curve cannot, and this curve represents the critical conditions for drop entrancement in water and corresponds to the lower boundary of the bubble entrainment region. When a vertical line is drawn across the critical curve, drop entrancement in water can be explained for fixed Fr and varying We numbers, i.e., at fixed drop diameter and velocity and varied drop temperature and surfactant concentration. For example, at point A below the curve, a drop cannot enter the water because of the high surface tension of water. If the surfactant concentration is increased, which reduces the water surface tension, the We number becomes larger and the position for the drop entrancement conditions in Fig. 10 rises. When the surfactant concentration reaches a certain value, it reaches the crossing point B of the curve and the line, at which point the drop can enter the water. On continuously increasing the surfactant concen-

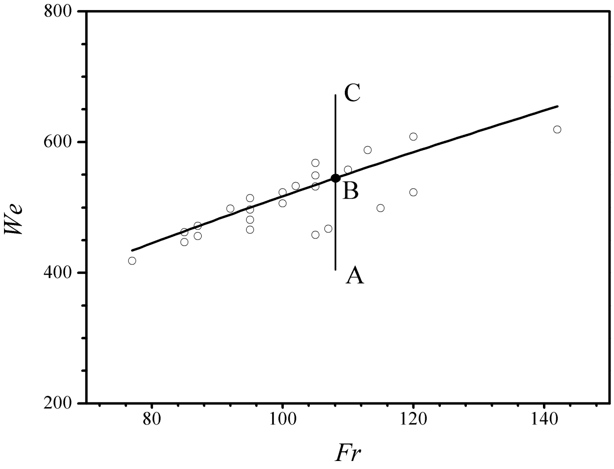

Figure 10. Drop critical entrancement conditions.

tration, i.e., decreasing the surface tension of water, the We number becomes larger and the position of the drop entrancement condition rises higher, i.e., at point C, drops can enter the water easily. In this case, the critical entrancement height for drops is lower. This is the physical meaning of the critical entrancement conditions.

What should be explained is that the interfacial tension between drop and water changes due to the addition of surfactant and affects the drop shape [9]. However, the drop entrancement is mainly determined by the cavity properties, which depends on the water surface tension, and the effects of shape change are little in the experimental conditions. So, the surface tension σ_c was used in the We number calculation.

3.3 Critical Entrancement Depth

It seems a little strange but does happen in the experiments that some drops which have sunk totally under the water still float up again, and drops that enter the water always sink to a deeper position under the water, which is deeper than the drop diameter. An analysis of the drop falling depth is helpful to understand the process of drop entrancement. The drop falling depth under the critical entrancement conditions is derived here. There must be a position under the water where the drop velocity is zero under the critical entrancement conditions, and the cavity size also reaches maximum. This depth of the drop is defined as the critical entrancement depth. Energy in the whole process has to be conserved, although the kinetic energy of the drop is transformed into gravity potential energy and surface energy of the cavity caused by collision [10]. It is assumed that the drop keeps its spherical shape without any change in the surface energy and there is no energy loss. This assumption is acceptable when drop deformation is negligible. Then,

$$E_k = E_g + E_s \tag{8}$$

where E_k is the kinetic energy of the drop, E_g the gravity potential energy, and E_s the surface energy of the cavity. According to Alexander et al. [10],

$$E_k = \frac{\rho_p \pi D_p^3}{12} U_p^2 \tag{9}$$

$$E_g = \pi \rho_c g R_m^4 / 4 \tag{10}$$

$$E_s = \pi \sigma_c R_m^2 \tag{11}$$

where ρ_p is the drop density of 4020, ρ_c the water density, R_m the maximal radius of the cavity (assumed to be hemispherical) which equals the critical entrancement depth, D_p is the drop diameter, U_p the drop velocity, and σ_c the surface tension of water. Several dimensionless parameters are first defined for simplifying the calculation:

$$l_p^* = [2\sigma_p / \left(\rho_p g\right)]^{1/2} / D_p \tag{12}$$

$$\rho^* = \rho_c / \rho_p, \qquad R_m^* = R_m / D_p \tag{13}$$

where l_p^* is the dimensionless capillary length, ρ^* the relative density and R_m^* the relative maximal radius. An expression from all the equations above is obtained as:

$$R_m^* = \left(l_p^* / \rho^{*1/2}\right) \left[\left(1 + \frac{2\rho^*}{l_p^{*2}} \frac{\mathrm{We}}{12\rho^*}\right)^{1/2} - 1 \right]^{1/2} \tag{14}$$

where the We number is:

$$\mathrm{We} = \frac{\rho_c U_p^2 D_p}{\sigma_c} \tag{15}$$

For the experimental conditions, it is calculated that $R_m^* = 2.3\text{~}2.5$, i.e., $R_m = 2.3\text{~}2.5 D_p$. This indicates that the critical entrancement depth is about 2.3–2.5 times the drop diameter. Although this result is a little larger than the observations in the experiments, it does confirm that the drop which can enter the water always falls to a deeper position than its diameter. The neglect of energy loss and shape change of the cavity during the drop fall may be the cause of the difference.

3.4 Mechanism of Drop Entrancement and Bubble Phenomena

Morton [8] and Rein [11] reported that the transformation from the shallow crater to bubble entrainment depends on the position of the cavity surface's first collapse in the situation of a water drop falling in water. In the shallow crater region, the cavity is nearly hemispherical which results in a water recovery starting from the bottom where the potential energy is the highest. In the case of bubble formation, the position with the highest potential energy or pressure around the cavity surface changes and is somewhere on the wall above the bottom. The bottom of the cavity is still moving downward when the cavity wall begins to move inward, producing a bubble under water.

Thus, the mechanism for drop entrancement and bubble phenomena can be suggested. First, when the drop kinetic energy is small and the corresponding cavity is small, the position with the highest pressure is always concentrated at the bottom of the cavity. Although the top of the drop is below the water surface, the cavity recovery begins from the bottom, which makes the drop rise again, as shown in Fig. 11. There is no bubble in this case and water from all other positions except the bottom is moving outside, e.g., the upper surface of

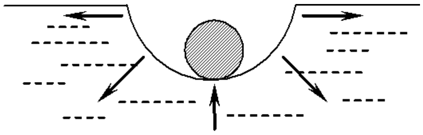

Figure 11. Cavity recovers from the bottom (arrows show the direction of water movement).

the water of the cavity spreads outside as waves rather than flowing inside to submerge the drop [10]. That is the reason why a drop below the water surface can rise again and the critical entrancement depth is larger than the drop diameter.

With the increase in the drop kinetic energy, the volume of the cavity increases. Under critical entrancement conditions, the cavity is nearly cylindrical and the position with the highest pressure changes from the bottom to a place above the bottom and the drop, and it collapses first and moves inward, as shown in Fig. 12. This motion performs a "closing" effect that seals off the drop under water. If the closing speed is fast enough, the drop is immersed in the water.

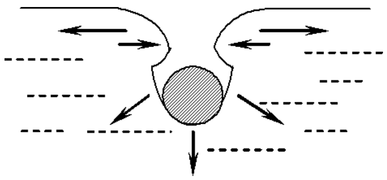

Figure 12. Cavity collapse from a position above the bottom (arrows show the direction of water movement).

In the "closing" process, there are often some bubbles together with the drop. If a bubble adheres to the top of the drop, it might make the drop rise. If the drop sinks down with a high speed, the bubble might separate from the drop and rise to the water surface. If the "closing" effect is not fast enough, there will be no bubble formed. The above explanations agree well with the observations in the experiments. It can be concluded that whether a drop can enter water properly depends on whether there is the "closing" effect on the cavity. If the "closing" effect is present and the closing speed is fast enough, the drop enters the water. If the "closing" speed is not fast enough, the drop is not sealed off and may rise again. Whether a drop with bubble rises or falls also depends on the volume of the bubble. If there is a small bubble sinking together with the drop, it might separate from the drop because of water turbulence. The essence of the closing effect is that the cavity collapses first from a position above the bottom where the pressure is the highest.

In this discussion, the influence of drop viscosity and its relation to granule shape is neglected. For the system of dispersed drops entering a continuous medium, the viscosity ratio, μ_p/μ_c is used to evaluate the influence on the drop shape. When $\mu_p/\mu_c < 1$, the drop is easily to be stretched and cracked, and when $\mu_p/\mu_c > 1$, the drop deformation can be neglected [9,12]. For rubber antioxidant 4020 and water system, $\mu_p/\mu_c > 1$, e.g., at 46 °C, $\mu_p = 95.6$ mPa/s, $\mu_c = 60.3$ mPa/s. So, the drop is considered to be spherical in discussing the entrancement process. Besides, drop solidification mainly occurs during the falling process in water, in which the drop already recovers to spherical shape. Therefore, the viscosity little affects the granule shape.

4 Conclusions

A new granulation technology for producing spherical particles was developed. Experiments were carried out with rubber antioxidants 4020 and 4010NA. Spherical particles of antioxidant 4020 and 4010NA with a uniform size were obtained. The granulation flow path is short with a high efficiency and simple equipment, and it is environmentally benign.

Drop entrancement is the crucial process in the granulation design. This mainly depends on the surface tension of water and the drop falling heights. A lower surface tension and higher falling height helps a drop enter the water. The critical entrancement condition depends on the drop velocity, drop temperature and surfactant concentration, which were derived as a power function of the We and Fr numbers.

Acknowledgements

The authors wish to express their appreciation of the financial support of this study by Sinorgchem Company Limited in Shandong Province, and to Yuan-Zhou Xi and Zhong-Dan Li for their help with the experiments.

Symbols used

D	[mm]	diameter of water drop
D_p	[mm]	diameter of 4020 drop
E_g	[J]	gravity potential energy of cavity
E_k	[J]	kinetic energy of drop
E_s	[J]	surface energy of cavity
Fr	[–]	Froude number
g	[m/s^2]	gravity acceleration
Hc	[cm]	critical entrancement height
l_p^*	[–]	dimensionless capillary length
R_m	[mm]	maximal radius of cavity
R_m^*	[–]	relative maximal radius of cavity
S	[–]	spreading coefficient
U	[m/s]	water drop velocity
U_p	[m/s]	drop velocity
We	[–]	Weber number

Greek symbols

α	[–]	constant
β	[–]	constant
γ_c	[mN/m]	surface tension of continuous phase
γ_p	[mN/m]	surface tension of dispersed phase
γ_{cp}	[mN/m]	interfacial tension between continuous and dispersed phases
μ_c	[mPa/s]	viscosity of continuous phase
μ_p	[mPa/s]	viscosity of dispersed phase
σ	[mN/m]	surface tension of water

σ_c	[mN/m]	surface tension of AEO7 solution
σ_p	[mN/m]	surface tension of drop
σ_{cp}	[mN/m]	interfacial tension between solution and drop
ρ	[g/cm^3]	water density
ρ_p	[g/cm^3]	drop density
ρ_c	[g/cm^3]	density of AEO7 solution
ρ^*	[–]	relative density

References

[1] Rubber Institute of the Chemical Industry and Engineering Society of China, *Handbook of Rubber Assistants* (Chinese), Chemical Industry Press, Beijing, China **2000**.

[2] G.-H. Zhao, D.-J. Ren, J.-Z. Li, *China Petrol. Chem. Eng.* **2005**, *4*, 44.

[3] J.-Y. Fang, Y.-Z. Xi, T.-J. Wang, Y. Jin, *Chem. Eng. Technol.* **2004**, *27 (9)*, 1039. DOI: 10.1002/ceat.200402036

[4] Y.-Z. Xi, T.-J. Wang, X. Li, Y. Jin, *Chem. Eng. Technol.* **2005**, *28 (6)*, 712. DOI: 10.1002/ceat.200407093

[5] F. M. Fowkes, *Adv. Chem. Ser.* **1964**, *43*, 99.

[6] C. Liu, J.-H. Li, *Surfactants Utility Handbook* (Chinese), Chemical Industry Press, Beijing, China **2004**.

[7] H. N. Oguz, A. Prospertti, *J. Fluid Mech.* **1990**, *219*, 143.

[8] D. Morton, M. Rudman, L. Jong-Leng, *Phys. Fluids* **2000**, *12 (4)*, 747.

[9] G. I. Taylor, *Proc. R. Soc. London, Ser. A* **1932**, *138 (834)*, 41.

[10] A. I. Fedorchenko, A.-B. Wang, *Phys. Fluids* **2004**, *16 (5)*, 1349.

[11] M. Rein, *J. Fluid Mech.* **1996**, *306*, 145.

[12] Z.-M. Li, W. Yang, B.-H. Xie, M.-B. Yang, et al., *Polym. Mat. Sci. Eng. (Chinese)* **2003**, *19 (5)*, 168.